Novel design and simulation of a hybrid solar electricity system with organic Rankine cycle and PV cells

Jing Li, Gang Pei*, Yunzhu Li and Jie Ji*

Department of Thermal Science and Energy Engineering, University of Science and Technology of China, 96 Jinzhai Road, Hefei City, Anhui Province, People's Republic of China

Abstract

The proposed system mainly consists of flat-plate compound parabolic concentrators (CPCs) integrated with photovoltaic (PV) cells and organic Rankine cycle (ORC). The technologies of CPC, PV cell and ORC are analyzed, and feasibility of the hybrid solar electricity system is demonstrated. Novel configuration for the hybrid electricity generation is carefully designed to react to different operating conditions. Fundamentals of the innovative system are illustrated, and mathematical models are developed to study the heat transfer and energy conversion processes. The results indicate that the low-temperature solar thermal power generation integrated PV cells can produce much more electric per unit surface area than side-by-side PV panels and CPC–ORC modules.

Keywords: solar electricity generation; organic Rankine cycle; photovoltaic cell; compound parabolic concentrator

*Corresponding authors:
peigang@ustc.edu.cn;
jijie@ustc.edu.cn

Received 12 May 2010; revised 21 June 2010; accepted 30 June 2010

1 INTRODUCTION

The majority of the solar radiation on the photovoltaic (PV) cell is converted into heat, and the PV cell efficiency becomes lower due to the increment of operating temperature. To overcome this limitation, hybrid photovoltaic/thermal (PV/T) technology is favorably adopted. The PV/T modules utilize electricity and heat simultaneously. Jie *et al.* proposed a novel PV/T. Performance tests were conducted, and the results showed that the system had a superior coefficient of performance for heat supply and the PV efficiency was also higher [1]. Pei *et al.* [2] presented the study of the influence of a glass cover on the PV/T system in terms of photothermic conversions and heat temperature. Previous research also focused on the selectivity of the absorber plate and PV cells of PV/T system. Gard *et al.* [3] analyzed the performance of a PV/T collector with integrated compound parabolic concentrator (CPC) troughs and pointed out that the system performed better on the use of selective absorber due to reduction in radiative heat losses from the absorber to glass cover. Hegazy *et al.* [4] investigated the performances of four PV/T solar air collectors and suggested that should the main objective of PV/T collectors be to provide sufficient electrical energy, the selective properties would be inappropriate for those PV/T collectors because of the resultant reduction in the generated PV electricity.

Although the topic of PV/T has attracted great attention, mainstream PV/T systems provided low-grade heat for domestic hot water supply or house heating. Electricity was produced solely by PV cells. However, electricity production will be increased when the temperature of collected heat is high enough for thermal power conversion. One way to increase the working temperature of the PV/T system is using a selective absorber or concentrated collector. Contini *et al.* [5] presented the selection of PV cell materials and manufacturing processes able to withstand the high-temperature conditions typical of interplanetary space missions toward the Sun. Meneses-Rodriguez *et al.* performed the experimental and theoretical analyses of the efficiency of high-temperature operation of a PV cell. It was concluded that amorphous silicon (α-Si) and CIS Schottky cells could operate at relatively high temperature (100–200°C) without drastic loss at their efficiency. And by coupling the high-temperature cell with a Stirling engine in a two-stage hybrid system, the calculated total conversion efficiency could be as high as 35–40% [6].

This paper develops a new concept of the PV/T system with PV–CPC as the collector and organic Rankine cycle (ORC) as the heat-to-power conversion cycle. Unlike the

International Journal of Low-Carbon Technologies 2010, 5, 223–230

doi:10.1093/ijlct/ctq027 Advance Access Publication 3 August 2010

current PV/T-air or PV/T-water system, PV–CPC collectors are working at relatively high temperature and electricity is produced by both PV cells and ORC cycle. The feasibility can be evaluated on the following conditions:

(1) Among many well-proven technologies, ORC is one of the most favorable and promising methods for low-temperature applications. Compared with the steam Rankine cycle, the ORC is scalable to smaller unit sizes and higher efficiencies during cooler ambient temperatures, immune from freezing at cold winter nighttime temperatures and adaptable for conducting semi-attended or unattended operations [7]. In the case of a dry fluid, ORC can be employed at lower temperatures without requiring superheating. This results in a practical increase in efficiency over the use of the cycle with water as the working fluid [8]. ORC can be easily modularized and utilized in conjunction with various heat sources. Feasibility of the ORC technology is reinforced by high technological maturity of majority of its components, spurred by extensive use in refrigeration applications [9]. ORC for combined heat and power (CHP) system with hot-side temperature around 100°C was tested, and the results indicated that the electrical efficiency was 16% and the overall efficiency was about 59% [10].
(2) CPC collectors are non-imaging concentrators. Their potential as collectors of solar energy was highlighted by Winston [11]. Smaller concentration ratio CPCs were able to accept a large proportion of the diffuse radiation incident on their apertures and concentrated it without the need of tracking the Sun [12]. Rabl summarized over 3 years worth of research on non-evacuated CPC collectors. At lower concentration ratios (e.g. 3X), CPC performance may be substantially better than a double-glazed FPC above about 70°C while merely requiring semi-annual adjustments for year-round operation [13]. Saitoh compared a CPC collector with a conventional FPC and evacuated tube collector. Experimental results indicated that the CPC collector possesses excellent thermal performance for high-temperature thermal electric applications in which the steam temperature should be >120°C [14].
(3) Currently available solar cells are suitable for commercial missions such as communications satellites, weather satellites and earth-orbiting missions, for which the PV battery fluctuation may change from −200°C to 200°C [15]. Another application of high-temperature solar cells is concentrated solar power. It is critical to extend the temperature range of solar cell operation for above purposes. For further development of high-temperature solar cells, the main difficulty to overcome is that the loss of efficiency with temperature results in low solar cell performance [16]. On the other hand, the proposed hybrid solar electricity system may work at temperature around 100°C, the PV efficiency loss will not be drastic. And α-Si cell would be economically and technologically suitable for this application. α-Si cell has relatively low-temperature coefficients of maximum power generated, which is about 0.21%/°C. By using high-temperature silicone elastomer, α-Si cell could work at higher temperature and remain efficient, e.g. about 85% of the standard efficiency at 100°C. Some α-Si cells available on the market have already complied with qualification including high-temperature thermal cycle and damp-heat testing [17].

The objective of this paper is to illustrate the fundamentals of the low-temperature solar thermal electric generation integrated PV cells and establish mathematical models for heat transfer and power conversion. The system performance is simulated based on distributed parameters, and the overall electricity efficiency is evaluated.

2 STRUCTURE AND FUNDAMENTALS

Figure 1 is the scheme of innovative design of the proposed system. The system mainly consists of hybrid PV–CPC modules and the ORC subsystem. Figure 2 shows the cross-section of the hybrid PV–CPC module. The PV cells are packed between two transparent layers, with an intermediate layer of high-temperature silicone elastomer. The whole lot of PV cells and transparent layers is pasted over a black absorber. Metallic panel-groove is put underneath the absorber to improve heat conduction and the working fluid tube is sealed between the panel-groove and the absorber. The adhesion process should be under precise pressure control to ensure good-quality thermal conductance. The ORC subsystem consists of a fluid storage tank with a phase change material (PCM) and turbine, generator (G), regenerator (R), condenser and pumps. The working fluid (generally organic) is vaporized in the tube of PV–CPC module under high pressure. The vapor flows into the turbine and expands, thus exporting power due to the enthalpy drop. The outlet vapor is first cooled down in the regenerator and further condensed to the liquid state in the condenser. The liquid is pressurized by pump 1, warned in the regenerator and then sent back to the tube. In contrast to a traditional solar Rankine system, there is an organic fluid storage tank with PCM instead of heat storage in this new design concept of thermal electric subsystem. The other novel characteristic is that two-stage collectors are employed. The key advantages of the configuration are the following: (1) there are conduits filled with PCM in the fluid storage tank, so the stability of the ORC subsystem will be guaranteed. (2) In order to strengthen the heat transfer performance in the second-stage collectors, the mass flow rate of the organic fluid can be increased by pump 2. Superheating of the organic fluid at the outlet of the collectors could be avoided. (3) Without any complicated controlling device, the process of heat storage or heat release can take place while electricity is being generated (storing heat if

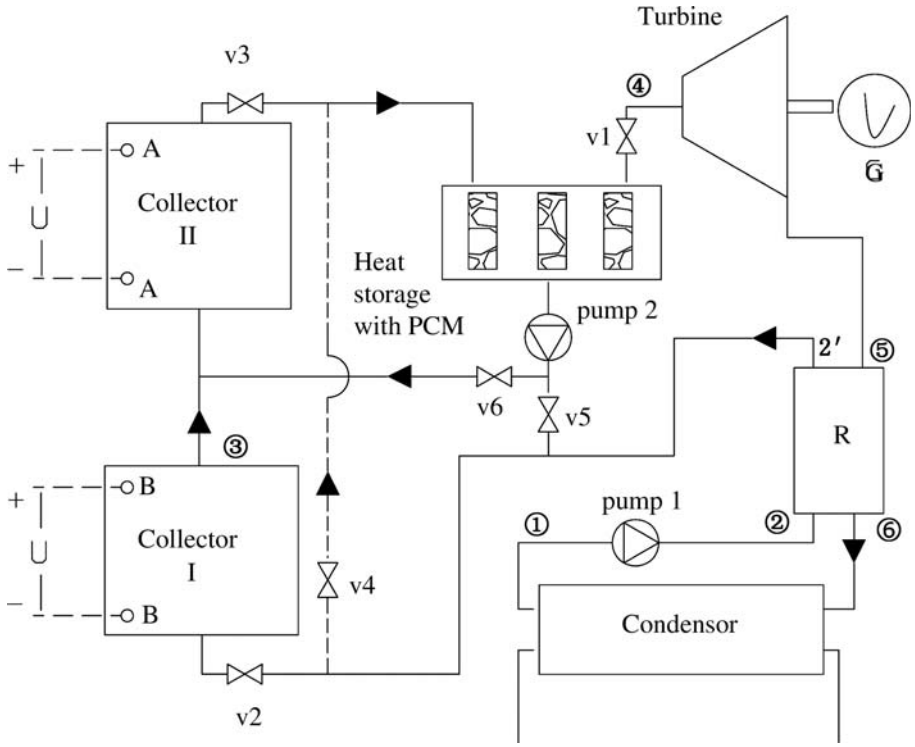

Figure 1. *Hybrid solar electricity system with ORC and PV cells.*

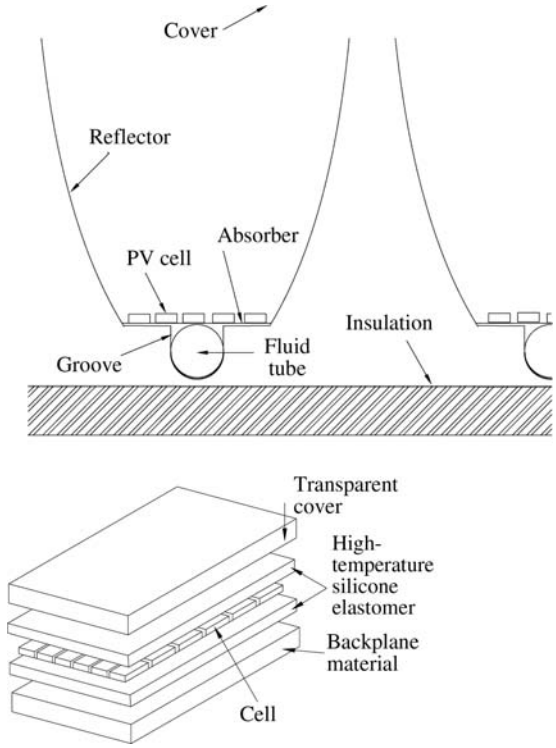

Figure 2. *Cross-section of the PV–CPC module.*

irradiation is strong, whereas releasing heat if irradiation is weak). On the use of pump 2, the system can run steadily and effectively in a wide irradiation range.

The hybrid solar electricity system will be set in three basic operation modes. In Mode I, valves 1, 2 and 3 are open. Pump 1 is running. Valve 6 may be open while pump 2 may run to prevent superheating in the second-stage collectors when irradiation is strong. Electricity is generated by both ORC and PV cells. In Mode II, valves 2, 3 and 5 are open. Pump 2 is running. Electricity is generated by PV cells and heat is stored by the PCM. In Mode III, valves 1 and 4 are open. Pump 1 is running. Heat is released and electricity is generated by the ORC.

3 MATHEMATICAL MODEL

In this section, mathematical model for heat transfer and power conversion of the hybrid solar electricity system is established. Equations are first developed for single PV–CPC module as illustrated in Figure 2. And the system modeling with PV–CPC modules in series is presented consequently.

3.1 Radiative heat transfer in the PV–CPC module

The total radiative heat loss from the PV absorber can be written in terms of A_S, T_S and T_L [18]:

$$q_{\text{rad S}\rightarrow\text{R+L}} = \varepsilon_{\text{eff}} A_S \sigma (T_S^4 - T_L^4) \quad (1)$$

$$\varepsilon_{\text{eff}} = \frac{\varepsilon_{\text{eff SL}} + \varepsilon_{\text{eff SL}}\varepsilon_{\text{eff RL}}}{\varepsilon_{\text{eff SL}} + \varepsilon_{\text{eff RL}}} \quad (2)$$

where $\sigma = 5.67 \times 10^{-8}\text{W/(m}^2\text{K)}$ is the Stefan–Boltzmann constant; A_S the absorber area, m^2; ε_{eff} the effective emissivity.

The subscript of S, L or R represents the absorber, glass cover or reflector, respectively, and SL or RL means radiative heat transfer between two surfaces. The emissivity of PV cells and the absorber is assumed to be uniform.

3.2 Convective heat transfer in the PV–CPC module

The overall convective heat transfer through the air inside the CPC is given by [19].

$$q_{\text{conv SL}} = A_S U_S \Delta T_S \tag{3}$$

$$U_S = \left[\frac{g\beta}{\nu^2} w^3 \Delta T_S Pr\right]^a \times c \times (k/w) \tag{4}$$

$$\Delta T_S = \frac{T_S - T_L}{1 + C^{-0.6}}$$

where U_S is the heat transfer coefficient for the absorber surface, W/(m^{2}K); ΔT_S the temperature differences across the air film at the absorber surface S; k the conductivity, W/(m K); w the length of the absorber, m; Pr the Prandtl number; a and c are constants for which the values have been suggested by [20]; g is earth's acceleration, m/s^2; β the volume coefficient of expansion, K^{-1}; ν the kinematic viscosity, m^2/s; C is the concentration ratio. Heat flow rate from L to the ambient is calculated by

$$q_{L-a} = \varepsilon_L A_L \sigma(T_L^4 - T_{Sky}^4) + A_L U_a (T_L - T_{air}) \tag{5}$$

3.3 Energy balance

Figure 3 shows the thermal energy network for a single PV–CPC module. The total irradiation absorbed by a single PV–CPC module is

$$q_{S,sol} = G A_L \gamma \tau_L \rho_{R,sol} \alpha_{S,sol} \tag{6}$$

where G is the irradiation density, W/m^2; γ the fraction of total irradiation accepted by the CPC; τ_L the solar transmissivity of cover; $\rho_{R,sol}$ the solar reflectivity of the reflector; $\alpha_{S,sol}$ the solar absorptivity of PV cells and absorber. And various energy fluxes are given by

$$\begin{aligned} q_{L-a} &= h_{L-a} A_L (T_L - T_a) \\ &= \varepsilon_L A_L \sigma(T_L^4 - T_{Sky}^4) + A_L U_a (T_L - T_{air}) \end{aligned} \tag{7}$$

$$\begin{aligned} q_{S-L} &= h_{r,S-L} A_S (T_S - T_L) + h_{c,S-L} A_S (T_S - T_L) \\ &= \varepsilon_{eff} A_S \sigma(T_S^4 - T_L^4) + A_S U_S \Delta T_S \end{aligned} \tag{8}$$

$$q_{S-f} = h_{S-f} A_f (T_S - T_f) \tag{9}$$

$$q_{f-a} = U_{f-a} A_f (T_f - T_a) \tag{10}$$

A_f is the heat transfer area of the tube; U_{f-a} the coefficient for heat loss through the insulation material; $h_{r,S-L}$ the radiative heat transfer coefficient; and $h_{c,S-L}$ the convective heat transfer coefficient.

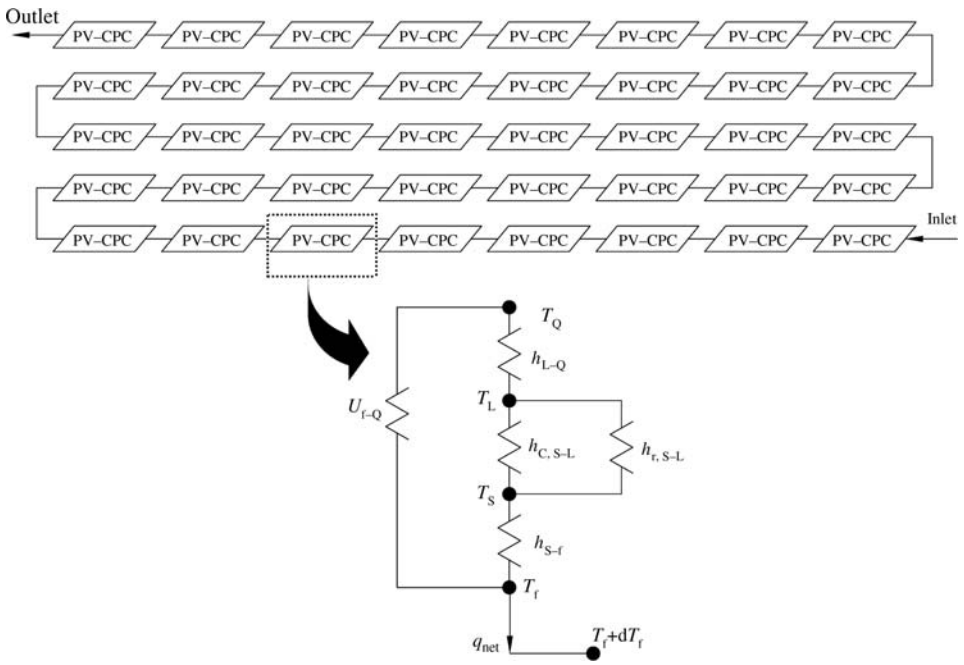

Figure 3. *Thermal energy network for single PV–CPC module and connection of PV–CPC modules in series.*

The steady-state energy equations for the cover L, absorber and PV cell S, and working fluid can be expressed by.

$$q_{L-a} - q_{S-L} = 0 \tag{11}$$

$$q_{S,sol} - q_{S-L} - q_{S-f} - p_{cell} = 0 \tag{12}$$

$$q_{S-f} - q_{f-a} - q_{net} = 0 \tag{13}$$

Heat transfer from the absorber to working fluid is calculated by

$$q_{S-f} = U_{tube}\pi D(T_S - T_f) \tag{14}$$

where U_{tube} is the heat transfer coefficient between the wall and working fluid, W/m^2 K; D the diameter of the tube. U_{tube} is calculated according to Ref. 18.

Electricity generated by PV cells is obtained by

$$p_{cell} = GA_L \times \eta_{PV}(T) \times x \tag{15}$$

where x is the cover ratio of PV cells.

$$\eta_{PV}(T) = \eta_{pv,0} - P(T - 25)\eta_{pv,0} \tag{16}$$

where $\eta_{pv,0}$ is the maximum PV efficiency on condition of AM1.5, 1000 W/m^2, 25°C; P is the temperature coefficient of the maximum power generated, °C^{-1}. The collector efficiency with net heat available for the working fluid is

$$\eta_c(T) = \frac{q_{net}}{GA_L} \tag{17}$$

Solar electricity system may demand tens or hundreds of collectors in series, and the temperature differences between neighboring collectors will be small. Thus, it is reasonable to assume the following [21]: (1) the average operating temperature of the PV–CPC changes continuously from one module to anther module; and (2) the function of the simulated area of the collector system is integrable. PV–CPC modules in series are shown in Figure 3 as an example. The differential equation for PV–CPC collector area and working fluid enthalpy increment is expressed by

$$q_{net} = \eta_c(T_S)GdA_L = m_f C_{p,f}(T_f)dT_f \tag{18}$$

$$\eta_c(T_S)GdA_L = m_f(H_{f,v} - H_{f,l})dY \tag{19}$$

Equation (18) is for liquid region and Equation (19) for binary region of the working fluid. Where m_f is the mass ratio, kg/s; $C_{p,f}$ the heat capacity, J/kg/K; $H_{f,v}$ or $H_{f,l}$ the enthalpy of the saturated vapor or saturated liquid, J/kg; and Y the dryness.

The key points of the simulation method for heat transfer of the hybrid solar electricity system are explained in detail in the Appendix.

3.4 Calculation of thermodynamic cycle

HCFC-123, a dry, environment-friendly [22] fluid that can prevent two-phase state during expansion without superheating, is selected as ORC fluid in this paper. Figure 4 shows the scheme of the thermodynamic cycle of HCFC-123. Point 1 shows the state of HCFC-123 at the condenser outlet; point 2 at pump 1 outlet; point 2′ at the regenerator outlet; point 3 at the first-stage collector outlet; point 4 at the turbine inlet; point 5 at the turbine outlet; and point 6 at the condenser inlet. The points referred in Figure 4 are put in Figure 1 with circles outside the numbers (except for 2′). The reversible processes of pressurization and expansion are described by 2s, 5s.

The practical efficiency can be calculated by

$$\eta_{orc} \approx \frac{(H_{5s} - H_4) \times \varepsilon_t \times \varepsilon_g - v_1(p_2 - p_1)/\eta_p}{H_4 - H_{2'}} \tag{20}$$

ε_t or ε_g is the turbine or generator efficiency. Since the heat capacity of HCFC-123 at point 2 is higher than that at point 5, the enthalpy at point 2′ should be calculated by [23]

$$H_{2'} = H_2 + [H_5 - H_{6(T_6=T_2)}] \times \varepsilon_r \tag{21}$$

ε_r is the regenerator efficiency. The enthalpy at point 6 in Equation (21) is obtained by assuming $T_6 = T_2$.

3.5 Equations developed for overall electricity efficiency

The overall system electricity efficiency is the sum of PV and thermal generated electricity divided by the total solar radiation.

$$\eta_e = \frac{1}{S}\left(\int_0^S \eta_{PV}(T) \times x dA_L + \eta_{orc}\int_0^S \eta_c(T)dA_L\right) = \bar{\eta}_{PV} \times x + \bar{\eta}_c \times \eta_{orc} \tag{22}$$

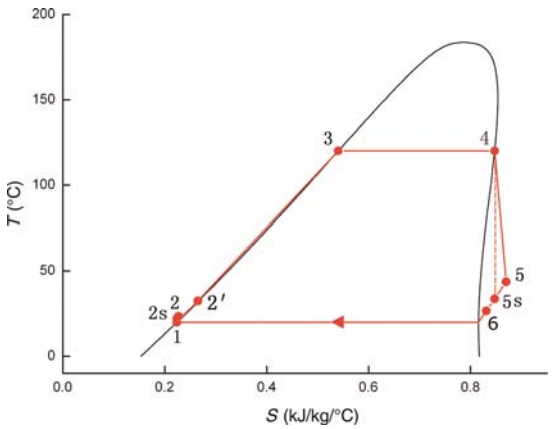

Figure 4. *Thermodynamic cycle of HCFC-123.*

Where S is the total area of PV–CPC modules; $\bar{\eta}_{PV}$ or $\bar{\eta}_c$ is the average PV efficiency or average collector efficiency of the PV–CPC modules.

4 SIMULATION RESULTS

The specifications of the hybrid solar electricity system with ORC and PV cells are listed in Table 1.

Figure 5 shows the ORC efficiency η_{orc} and average collector efficiency $\bar{\eta}_c$ variation with HCFC-123 evaporation temperature. According to the second law of thermodynamics, the ORC efficiency is improved by larger temperature difference between the hot and the cold sides. However, the collector efficiency becomes lower when the average working temperature rises. Since the working fluid is heated from condensation temperature to evaporation temperature, the average working temperature of the collectors is lower than HCFC-123 evaporation temperature.

Figure 6 shows the average PV efficiency $\bar{\eta}_{PV}$ and system electricity efficiency η_e variation with HCFC-123 evaporation temperature. The average PV efficiency becomes lower when the evaporation temperature rises. On the other hand, the system electricity efficiency first climbs up and then falls down with the increment of evaporation temperature. This can be explained according to Equation (22). The increment of evaporation temperature has negative influences on the average PV efficiency and average collector efficiency but has positive ones on the ORC efficiency. Owing to this tradeoff, there is a maximum value for the system electricity efficiency η_e. When the evaporation temperature is 118°C, the system electric efficiency is 13.1%, nearly two times higher than the PV efficiency at room temperature. The $\bar{\eta}_{PV}$ curve shows a similar tendency to the $\bar{\eta}_c$ curve. The slope of the $\bar{\eta}_{PV}$ curve is smaller than the defined temperature coefficients of the maximum power generated of PV cell, e.g. at the point of evaporation temperature of 120°C, the tangent slope of the $\bar{\eta}_{PV}$ curve is 0.14%, about two-thirds of the temperature coefficients listed in Table 1 (0.21%). This is because that in the electric generation system, the temperature of one PV–CPC module is different from another. The average operating temperature of the PV–CPC modules is determined both by the working temperature range and by the distribution of lower and higher temperature modules.

Table 1. Specifications of parameters for simulation.

Parameters	Value	Parameters	Value
Irradiation G, W m^{-2}	1000	Working fluid	HCFC-123
Environment temperature, °C	20	Absorber emissivity	0.1
PV standard efficiency $\eta_{pv,0}$	7.27%	Absorber absorptivity	0.9
PV temperature coefficient P, °C^{-1}	0.21%	Tube diameter D, m	0.025
PV–CPC module absorber length, m	0.05	Pump efficiency η_p	0.75
Mass flow rate m_f, kg/s	0.2	Turbine efficiency ε_1	0.85
Concentration ratio of CPC	4.9	Generator efficiency ε_2	0.95

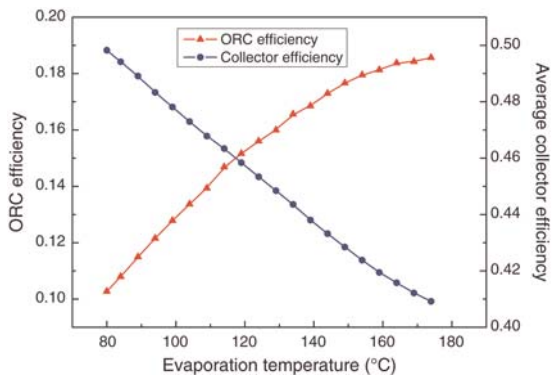

Figure 5. *ORC and average collector efficiency variation with the working fluid evaporation temperature.*

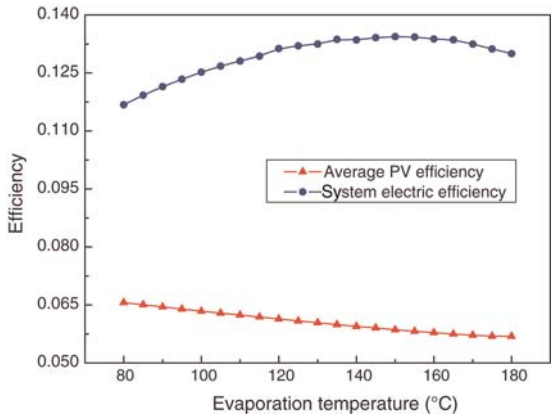

Figure 6. *Average PV and system electric efficiency variation with the working fluid evaporation temperature.*

5 ECONOMIC ANALYSIS

The technology of hybrid PV/T systems for conversion of solar energy with simultaneous production of electricity and thermal energy has been developing. The domestic market for the systems in both EU and China is large. PV/T collectors are now commercially available and manufactured in growing quantities. A lot of experience on the PV/T module as well as system level has been obtained. In order to get a primary understanding of the economic performance of the proposed low-temperature solar thermal electric generation integrated PV cells, the characteristic aspects are analyzed as follows in comparison with mainstream PV/T-water or PV/T-air systems.

(1) An expander, working fluid pump, condenser and heat storage unit is needed in the hybrid solar electricity system. In mature, cost-optimized large-volume industries, the cost of products is proportional to the weight of materials used [24]. The cost of the expander and pump will be negligible when compared with that of collectors

and heat storage in large-scale manufacturing because the consumed materials of the latter devices are strongly correlated with the installed capacity. On the other hand, the additional cost of the hybrid solar electricity system for heat storage is only a replacement of electricity storage cost since storage batteries become dispensable. The capital cost may be competitive with that of the current PV/T-water or PV/T-air systems.

(2) Heat recovery from the working fluid at the turbine outlet could be carried out by the condenser. Thus, hot water supply or space heating is realized. The overall heat collection or PV efficiency of this kind of CHP system is lower than mainstream PV/T system efficiency due to the relative higher operation temperature, e.g. heat collection efficiency is 51.8% or 46.9%, respectively, when hot-side temperature of the working fluid is 60°C or 110°C, while the overall PV efficiency is 6.8% or 6.2%, respectively. However, the overall electricity efficiency is much higher, e.g. 12.8% when hot-side temperature of the working fluid is 110°C. Payback time of the proposed system is thereby expected to be shorter.

6 CONCLUSION

The configuration of the proposed low-temperature solar thermal electric generation integrated PV cells system is carefully designed. The feasibility can be qualitatively demonstrated under conditions of low-temperature coefficients PV cells, small concentration ratio CPC collectors and ORC cycle. The PV–CPC modules can generate more electricity per unit surface area than side-by-side PV panels and CPC collectors for thermal electric generation. When the evaporation temperature is 118°C, the system electricity efficiency is 13.1%, nearly two times as much as the PV efficiency at room temperature. The simulation results and technical analysis of existing solar cells, CPC and ORC indicate that the hybrid solar electricity generation is promising.

ACKNOWLEDGEMENTS

This study was supported by the National Science Foundation of China (Project Numbers: 50974150, 50978241 and 50708105) and the National High Technology Research and Development Program of China (863 Program) (Project Number: 2007AA05Z444).

APPENDIX: CALCULATION OF HEAT TRANSFER IN THE PV–CPC COLLECTORS

The known conditions:

(1) mass flow rate of HCFC-123 m_f;
(2) PV–CPC collectors inlet temperature of HCFC-123 $T_{f,0}$;
(3) total PV–CPC collectors area S;
(4) irradiance G and environment temperature T_a.

The unknown conditions:

(1) PV–CPC collectors outlet temperature of HCFC-123 $T_{f,o}$ (liquid state) or the dryness $Y_{f,o}$ (binary state);
(2) average PV efficiency $\bar{\eta}_{PV}$ and average collector efficiency $\bar{\eta}_c$

The controlling equations for the energy balance of HCFC-123 are Equations (18) and (19).

A numerical approach for computation of HCFC-123 temperature or dryness along the tube is adopted.

$$T_{f,n+1} = T_n + \frac{\eta_c(T_{S,n})G}{m_f C_{p,f,n}}\Delta A_L \tag{23}$$

$$Y_{f,n+1} = Y_n + \frac{\eta_c(T_{S,n})G}{m_f(H_{f,v} - H_{f,l})}\Delta A_L \tag{24}$$

Equation (23) is for liquid region and Equation (24) for binary region of HCFC-123. ΔA_L is the discrete area ($\Delta A_L = S/N$). The subscript n or $n+1$ is the discrete point. (The number of total discrete points is $N+1$.) The calculation procedure is

(I) Input a value of $T_{S,0}$ (absorber temperature of the first discrete point).
(II) Calculate T_L according to Equations (7, 8 and 11), and calculate q_{s-L} consequently. The area of A_L in the equations is replaced by ΔA_L.
(III) Calculate $q_{S,sol}$ q_{S-f} or p_{cell} according to Equations (6, 14 or 15), respectively.
(IV) The correct solution to T_{S0} must fulfill energy balance. If absolute value of $(q_{S,sol} - q_{S-L} - q_{S-f} - p_{cell})$ is smaller than f (judging parameter), then output $T_{S,0}$ (correct values). Otherwise go to step I and refine $T_{S,0}$.
(V) With $T_{S,0}$, q_{net} is calculated according to Equation (13) and $\eta_t(T_{S,0})$ is calculated according to Equation (17).
(VI) $T_{f,1}$ (liquid region) or $Y_{f,1}$ (binary region) is calculated according to Equation (23 or 24).
(VII) With $T_{f,1}$ or $Y_{f,1}$, $T_{f,2}$ or $Y_{f,2}$ is calculated in a similar way as steps I–VI.
(VIII) $T_{f,n+1}$ or $Y_{f,n+1}$ is calculated based on $T_{f,n}$ or $Y_{f,n}$ in the same manner until $T_{f,o}$ or $Y_{f,o}$.
(IX) Output $p_{cell,n}$, $q_{net,n}$ ($n = 0, 1, 2, \ldots, N$).
(X) The total electricity generated by the PV cell or ORC is $P_{PV} = \sum_1^N p_{cell,n}$ or $P_{orc} = \sum_1^N q_{net,n} \times \eta_{orc}$. And, the average PV efficiency or average collector efficiency is $\bar{\eta}_{PV} = P_{PV}/(xG\Delta A_L N)$ or $\bar{\eta}_c = \sum_1^N q_{net,n}/(G\Delta A_L N)$.

The flow charts are shown in Figure 7.

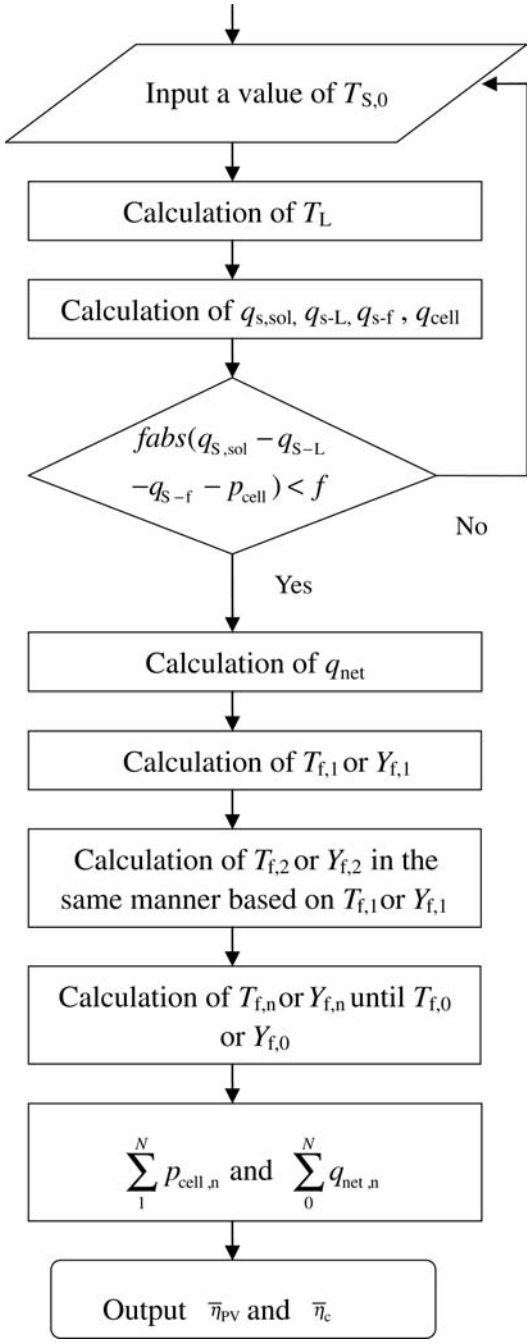

Figure 7. *Calculation method for average PV efficiency or average collector efficiency of the hybrid solar electricity system.*

REFERENCES

[1] Ji J, Pei G, Chow T-T, *et al*. Experimental study of photovoltaic solar assisted heat pump system. *Sol Energy* 2008;**82**:43–52.

[2] Pei G, Jie J, Chow T-T, *et al*. Performance of the photovoltaic solar-assisted heat pump system with and without glass cover in winter: a comparative analysis. *Proc IMechE: Part A: J Power Energy* 2007;**222**:179–187.

[3] Gard HP, Adhikari RS. Performance analysis of a hybrid photovoltaic/thermal (PV/T) collector with integrated CPC troughs. *Int J Energy Res* 1999;**23**:1295–304.

[4] Hegazy AA. Comparative study of the performances of four photovoltaic/thermal solar air collectors. *Energy Convers Manage* 2000;**41**:861–81.

[5] Contini R, Accoiti GD, Ferrando E, *et al*. Development activities of GaAs space solar cells and photovoltaic assemblies for high temperature applications. *Photovoltaic Specialists Conference, Conference Record of the Twenty-Ninth IEEE*, 2002, 808–11.

[6] Meneses-Rodriguez D, Horley PP, Gonzilez-Hernhdez J, *et al*. High temperature operation of photovoltaic solar cells in one- and two-stage systems. *1st International Conference on Electrical and Electronics Engineering*, 2004, 305–9.

[7] Prabhu E. Solar trough ORC. Subcontract report NREL/SR-550-39433, 2000.

[8] Andersen WC, Bruno TJ. Rapid screening of fluids for chemical stability in organic Rankine cycle applications. *IndEng Chem Res* 2005;**44**:5560–6.

[9] Quoilin S, Lemort V. Technological and economical survey of organic Rankine cycle systems. *5th European Conference Economics and Management of Energy in Industry*, 2009, 14–7.

[10] Riffat SB, Zhao X. A novel hybrid heat-pipe solar collector/CHP system—Part II: theoretical and experimental investigations. *Renew Energy* 2004;**29**:1965–90.

[11] Winston R. Principles of solar concentrators of a novel design. *Sol Energy* 1974;**16**:89–95.

[12] Pereira M. Design and performance of a novel non-evacuated 1.2x CPC type concentrator. *Proceedings of Intersol Biennial, Congress of ISES*, Montreal, Canada, 1985, 1199–204.

[13] Rabl A, O'Gallagher J, Winston R. Design and test of non-evacuated solar collectors with compound parabolic concentrators. *Sol Energy* 1980;**25**:335–51.

[14] Saitoh TS. Proposed solar Rankine cycle system with phase change steam accumulator and CPC solar collector. *37th Intersociety Energy Conversion Engineering Conference (IECEC)*, Paper No. 20150, 2002.

[15] Torchynska TV, Polupan G. High efficiency solar cells for space applications. *Superficies y Vacío* 2004;**17**:21–5. http://www.fis.cinvestav.mx/~smcsyv/supyvac/17_3/SV1732104.PDF.

[16] Landis GA, Jenkins P, Scheimant D, *et al*. Extended temperature solar cell technology development. *AIAA 2nd International Energy Conversion Engineering Conference*, 2004, 16–9. http://ntrs.nasa.gov/archive/nasa/casi.ntrs.nasa.gov/20050198962_2005199189.pdf.

[17] Ton D, Tillerson J, McMahon T, *et al*. *Accelerated Aging Tests in Photovoltaics Summary Report*. U.S. Department of Energy Efficiency and Renewable Energy, 2007.

[18] Incropera FP, Dewitt DP, Bergman TL, *et al*. *Fundamentals of Heat and Mass Transfer*, Xinshi G, Hong Y, trans., 6th edn. Chemistry Industry Press (Chinese), 2007.

[19] Rabl A. Optical and thermal properties of compound parabolic concentrators. *Sol Energy* 1976;**18**:497–511.

[20] Kreith F. *Principles of Heat Transfer*, 3rd edn. Intext Educational, 1973.

[21] Gang P, Jing L, Jie J. Analysis of low temperature solar thermal electric generation using regenerative organic Rankine cycle. *Appl Therm Eng* 2010;**30**:998–1004.

[22] Batchelor T. The global environmental benefit from the use of HCFC-123 in centrifugal chillers. http://www.unep.fr/ozonaction/information/mmcfiles/4921-e-HCFC-123_chillers.pdf.

[23] Cayer E, Galanis N, Desilets M, *et al*. Analysis of a carbon dioxide transcritical power cycle using a low temperature source. *Appl Energy* 2009;**86**:1055–63.

[24] Der Minassians A, Aschenbach KH, Sanders SR. Low-cost distributed solar-thermal-electric power generation. *ProcSPIE* 2004;**5185**:89–98.